A modified moiré interferometer for three-dimensional displacement measurement

Weining Wang (王卫宁)[1] and Jianhai Sun (孙建海)[2]

[1] *Department of Physics, Capital Normal University, Beijing 100037*

[2] *Institute of Electronics, Chinese Academy of Sciences, Beijing 100080*

Received February 13, 2004

This paper presents a new optical interferometric system, MMI-T/G, composed of a modified four-beam moiré interferometer and a Twyman/Green interferometer. The MMI-T/G system can measure three-dimensional displacement fringe patterns with a single loading on the specimen, and the in-plane and out-of-plane displacement fields can be measured independently and defined clearly. The optical setup has the advantages of structural novelty, flexibility, and high fringe contrast. Moreover, the in-plane displacement sensitivity is twice of that of the normal moiré interferometer. The measuring techniques to obtain the fringe patterns and displacement fields using the MMI-T/G system are described. The experimental results of thermal displacement of an electronic device are shown.

OCIS codes: 120.3180, 120.4120, 999.9999 (three-dimensional displacements).

In the last decade or so, some three-dimensional (3D) displacement measurement methods, which combined in-plane moiré interferometry (MI) with out-of-plane measurement techniques, such as Fizeau interferometry or Michelson interferometer, have been developed[1-4]. In those setups, auxiliary beam-splitting optical components, such as a large and highly collimated lens, diffractive grating (transmissive or reflective) or multi-terminal optic fibers, were used to separate one laser beam into several beams for two or four beams MI measurement. If the auxiliary optical components are imperfect, the wavefront coming from the auxiliary optical components will be warped, resulting in unwanted initial fringes to the interference pattern, as the specimen is loaded. Therefore there is an advantage in avoiding using the auxiliary optical components so as to reduce the complexity of the measurement system.

Lin proposed a 3D MI system[5]. In Lin's setup, the specimen grating diffracts the incident beam into several beams and re-diffracts those diffracted beams (each of them is reflected from a mirror back to the path of the incoming beam), therefore there is no need for auxiliary beam-splitting optical components. The re-diffracted beams propagate to the camera coaxially to generate a fringe pattern with uniform intensity. Lin's system has a simple structure and the in-plane sensitivity is twice of that of the normal MI. However, there are two major problems in using Lin's setup, one is that the fringe pattern representing the out-of-plane displacement is dependent on the in-plane displacement; the other is that the out-of-plane fringe sensitivity of the interferometer is relatively low.

A new optical system, MMI-T/G, which combines a modified in-plane MI with a Twyman/Green interferometry and can measure 3D displacement fringe patterns with a single loading on specimen, was setup. In the new setup, the fringe patterns of the out-of-plane and in-plane displacements are mutually independent. The sensitivity of the out-of-plane displacement is shown to be higher than that of Lin's setup.

Figure 1 shows a schematic arrangement of the MMI-T/G for measuring 3D displacements. The light from a laser is expanded and collimated by an object lens (OL) and a collimating lens (CL) respectively, then split into two beams by a beam-splitter (BS). Beam I impinges onto the specimen in line with the normal direction of the specimen, and beam II impinges onto the plane mirror (M). A crossed-line diffraction grating (1200 line/mm) is replicated on the surface of the specimen. Four plane mirrors, M_1, M_2, M_3, and M_4, are symmetrically mounted in front of specimen with an offset angle to the normal direction of the specimen, corresponding with the direction of ± 1 order diffractive beams, respectively. M_1 and M_2 are positioned in the x-z plane, providing the contour map of the in-plane displacement U (representing the x-displacement field), and M_3 and M_4 are positioned in the y-z plane, providing the contour map of the in-plane displacement V (representing the y-displacement field).

The surface of the plane mirror M is set perpendicular to the surface of the specimen, with the optical path length between M and BS being the same as that between the specimen and BS. This is a typical Twyman/Green

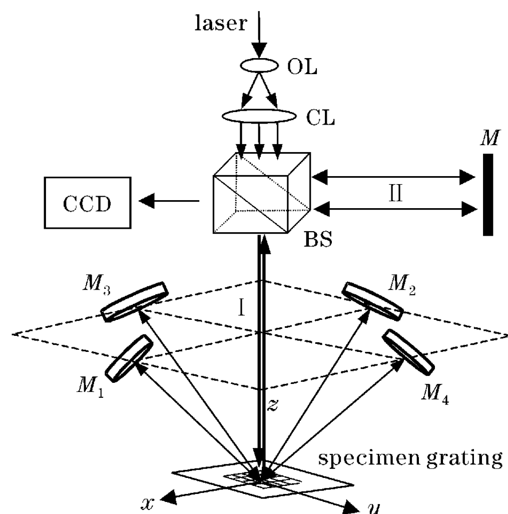

Fig. 1. Schematic arrangement of MMI-T/G for 3D deformation measurement. CCD: charge-coupled device.

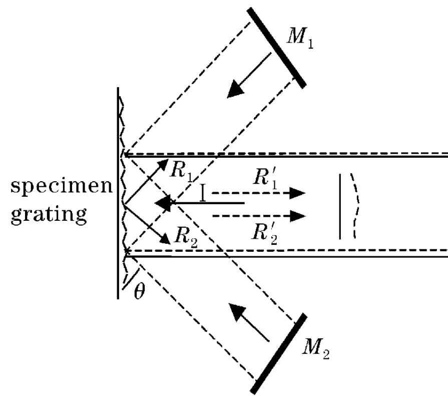

Fig. 2. MMI for U field measurement.

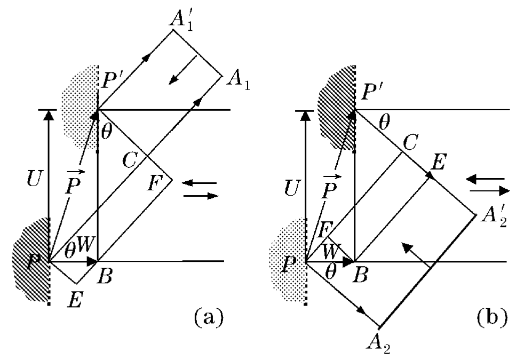

Fig. 3. Illustration of the path difference of light caused by 3D displacements. (a): Optical path of M_1; (b): that of M_2.

interferometry setup providing the complete interference as well as the contour map of the out-of-plane displacement W (representing the z-displacement field).

The simplified schematic of the optical path for measuring the in-plane displacement U field can be illustrated in Fig. 2. The incident beam (beam I, at the normal direction of specimen) is a plane wave. When the specimen is deformed under loading, the specimen grating is also deformed. Therefore the plane wavefronts (+1 and −1 order) diffracted from the specimen grating become warped wavefront R_1 and R_2. The diffractive angle θ is

$$\sin\theta = \lambda f. \tag{1}$$

After being reflected from M_1 and M_2, and then re-diffracted from the specimen grating, the +1 and −1 order wavefront, become warped wavefronts R_1' and R_2'.

Assuming a small deformation of the specimen under loading in three dimensions from P to P' as a vector $\vec{P}$, and U and W are displacement components of $\vec{P}$ in x- and z-direction, respectively, and assuming A_1 and A_1' are two points on the surface of M_1, the optical paths, which have been re-diffracted by M_1 before and after deformation, can be described as $B \to P \to A_1 \to P \to B$ and $P' \to A_1' \to P'$, respectively, as shown in Fig. 3(a). The difference in the light path diffracted by M_1 before and after deformation can be calculated as

$$\Delta_1 = 2(BP + PA_1) - 2P'A_1' = 2(U\sin\theta + W\cos\theta + W)$$

$$= 2[W(1+\cos\theta) + U\sin\theta]. \tag{2}$$

Similarly for M_2, as shown in Fig. 3(b), the difference in the light path diffracted by M_2 before and after deformation can be calculated as

$$\Delta_2 = 2[W(1+\cos\theta) - U\sin\theta]. \tag{3}$$

The two re-diffracted wavefronts, R_1' and R_2', interfere at the CCD target. The interference fringe occurs when

$$\Delta(x,y) = \Delta_2 - \Delta_1 = N_x\lambda, \tag{4}$$

where N_x is the order of the U field fringe.

Substituting Eq. (1) into Eq. (4), the displacement-fringe governing equation in the x-direction can be obtained as

$$U(x,y) = \frac{N_x}{4f}. \tag{5}$$

The displacement component $V(x,y)$ in the y-direction can be determined similarly, given as

$$V(x,y) = \frac{N_y}{4f}, \tag{6}$$

where N_y is the order of the V field fringe.

It can be seen that the in-plane displacement-fringe governing equations (Eqs. (5) and (6)) are similar to those of the conventional MI system, but the measurement sensitivity of the new method is doubled. In the case of $\lambda = 0.6328$ μm and $f = 1200$ line/mm, using this new method, the relative in-plane displacement is 0.208 μm per fringe order.

The out-of-plane displacement W field pattern is formed by the zeroth-order diffractive beam from the specimen grating interfering with the reference beam reflected from M. As well known, the out-of-plane displacement can be simply determined by

$$W = \frac{N_z\lambda}{2}, \tag{7}$$

where N_z is the order of the W field fringe.

The sensitivity of the out-of-plane displacement in the present MMI-T/G setup is $2/\lambda$. In the case of $\lambda = 0.6328$ μm and $\theta = 49.408°$ (for the +1 diffraction order when $f = 1200$ line/mm), the sensitivity of the out-of-plane displacement in this setup is 2.9 times of that obtained by Lin's. The relative out-of-plane displacement in this setup is 0.316 μm per fringe order.

Three displacement components in x-, y-, and z-directions are theoretically independent of each other, as shown in Eqs. (5)−(7). However, in practice, the fringe patterns of displacement fields U, V, and W may overlap in the CCD target if the re-diffracted beams travel along the same direction with that of the zeroth-order diffracted beam from the specimen grating. With the current setup, the two mirror pairs (M_3 and M_4 in x-y plane, and M_1 and M_2 in y-z plane) are adjusted with a very small offset angle (about 0.5°) to the direction of the ±1 order diffractive beams, respectively. So the re-diffracted beams from the specimen grating will also form with a similar small offset angle to the normal direction of the specimen in x-z and y-z plane,

respectively. Three fringe patterns are separated at the recording plane of CCD. Consequently, the same CCD target can be used to obtain the in-plane and out-of-plane fringe patterns independently.

The proposed MMI-T/G method has been applied to a testing case of an electronic package under thermal loading. The sample is a copper base of a semiconductor with two kovar leads. Epoxy glass is used to fill the gap between the leads and the base. The mechanical reliability resulting from the thermal displacement mismatch between the leads and the base is a critical issue. Therefore, the measurement of high accuracy, 3D and full field thermal deformation of the package copper base is necessary for package design and qualifications. The 3D displacements were measured by using the system shown in Fig. 1. A He-Ne laser ($\lambda = 0.6328$ μm) was used. The leads were cut and the surface of the specimen was mirror-like polished. A 1200-line/mm crossed-line grating was replicated on the specimen surface at room temperature. A thermo-chamber with an optical window was used to heat the specimen uniformly.

Figure 4 shows the U, V, and W fringe fields resulting from the deformed specimen, which was heated to different temperature in the thermo-chamber. The results show clear fringe contrast and illustrate that the distribution of the thermal strain in the base is not uniform due to the existence of the two leads. It can be seen that the thermal strains between the two leads are lower than those between other parts further away from them, and there are shear strains generated around these two kovar leads. Figure 5 shows the displacement and strain maps for the fringe patterns at 48 °C in Fig. 4. Some quantitative results, such as the in-plane displacement, the average in-plane strain, and out-of-plane warpage of the specimen, are calculated based on the resultant 3D fringe patterns and shown in Table 1. Average in-plane thermal expansion rate (based on in-plane displacement data induced by different level thermal loading) is 6.123×10^{-6} /°C. All these parameters provide the reliable data for designing and optimizing the structure and improving the reliability of the electronic packages.

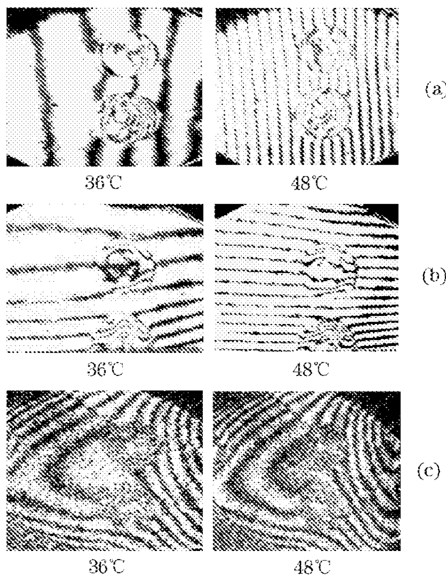

Fig. 4. 3D fringe patterns of the semiconductor base under different temperatures. (a): U field; (b): V field; (c): W field.

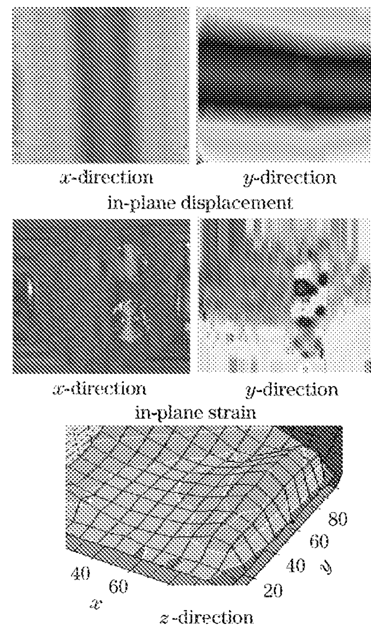

Fig. 5. Displacement and strain maps under the temperature loading of 48 °C.

Table 1. Experimental Date under Different Thermal Loading

Thermal Loading (°C)	In-Plane Displacement x-Direction (μm)	y-Direction (μm)	Maximum Convexity (μm)
36	1.04	1.25	1.89
48	3.74	3.12	2.21

In conclusion, the advantages of the new 3D optical displacement measurement system, MMI-T/G, can be summarized as follows. It not only can measure 3D displacement fringe patterns with a single loading on the specimen independently, but also can be flexibly set in measurements. Moreover, the in-plane displacement sensitivity of this system is twice of that of conventional MI. It can be used as an effective tool for studying the mechanical properties of materials and improving the design of substructure and the reliability of electronic packages.

The authors are grateful to the financial support by the Science and Technology Development Foundation, Education Commission of Beijing, P. R. China (No. 00KJ-094). Technical discussions with Dr. Y. Chen, Atkins (UK) are also acknowledged gratefully. W. Wang's e-mail address is wwn-phy@mail.cnu.edu.cn.

References

1. A. Asundi, M. T. Cheung, and C. S. Lee, Experimental Mechanics **29,** 258 (1989).
2. Y. Wang and F. P. Chiang, Opt. Eng. **33,** 2654 (1994).
3. J. A. Gilbert, R. L. Shepherd, H. J. Cole, and P. R. Ashley, Opt. Eng. **36,** 3336 (1997).
4. F. L. Dai, H. X. Shang, C. Li, and H. M. Xie, Proc. SPIE **5058,** 393 (2002).
5. S.-T. Lin, Opt. Eng. **40,** 822 (2001).